Analysis of Turbulence of Aluminium and Molten Cryolite in the Aluminium Electrolysis Cell

Mounir Baiteche[1], Seyed Mohammad Taghavi[2], Donald Ziegler[3], Samaneh Poursaman[4] Mario Fafard[5]
1. Postdoctoral fellow
2. Assistant professor
4. Master student
5. Professor
Aluminium Research Centre REGAL, Laval University, Québec, Canada
3. Program Manager-Modeling, Alcoa Primary Metals, Alcoa Technical Center, PA, USA
Corresponding author: mounir.baiteche.1@ulaval.ca

Abstract

The aluminium electrolysis cell used in Hall-Héroult process contains two stratified molten materials (aluminium and cryolite). These fluids are subjected to gravity, shear and high-intensity electromagnetic stresses. The two-fluid flow is important as it ensures distribution of alumina and heat throughout the cell; avoids depletion of reactants and local overheating. However, on the other hand, it is difficult to describe the flow of fluids at any time throughout the volume of the cell. The fluids are opaque, of high temperature and excessively aggressive and the cell is of complex geometry. It is very important to define the parameters that influence the flow of both fluids. In this article, a comparison is made to test different turbulence models to simulate the fluid flow in the cell. Different approaches using the Reynolds Averaged Navier-Stokes (RANS) and using the Large Eddy simulation (LES) method are compared. A simplified model of the electrolytic cell is considered for this purpose in order to investigate the transient fluctuations of the fluids velocity field in aluminium electrolysis cell.

Keywords: Aluminium electrolysis, two-phase flow, stratified fluids, magnetohydrodynamics of aluminium electrolysis cells, turbulence models.

1. Introduction

The Hall-Héroult process consists of the dissolution of alumina in an electrolytic bath. A high intensity electric current passes through the media resulting in the production of liquid aluminium which collects to the bottom of the cell. This reaction then produces a layer of molten aluminium at the bottom of cryolite bath at a temperature of around 960 °C [1]. On an industrial scale, this process is used in large cells, which can produce several tons of aluminium per day [2]. Liquid metal in the cell as well as the electrolytic bath where the different chemical reactions take place constitute a two-fluid system, in which, in addition to the chemical reactions, a certain number of thermo-solutal and magnetohydrodynamic phenomena occur [3]. The magnetic field is produced by the main current through which the cell is fed as well as the neighboring cells and magnetized steel parts [4]. The two fluids present in the cell are conductive to the electric current. Their movement within a magnetic field causes the induction of a non-negligible electric current and thus participates in the magnetism produced in and around the cell.

Fluid-flow of the bath is essential for the dispersion and the dissolution of the alumina and the distribution of the chemical species in the bath [4]. The chemical kinetics of the reactions is also influenced by the flow. The reaction rate is increased by the flow and the mixing caused by the velocity field achieves high reaction levels. The thermal balance of the cell is also influenced by the fluid flow [5]. However, the intensity of the flow must remain in a certain range to ensure

stability of the cell. High velocity fields can alter the proper functioning in terms of safety and energy efficiency of the electrolysis process. The fluctuating instabilities of the fluids in the cell go along with the modification of the shape of the interface between the aluminium and the cryolitic bath. This deformation changes the local distance between the anodes and the surface of the aluminium layer and thus the current distribution [6]. This change in distribution will typically reduce the cells performance [7].

Controlling the flow of the fluids in the electrolysis cell is very important, although it is difficult to observe the different flow regimes during its operation. Thus, an approach is based on numerical simulations to predict the behavior of the two stratified fluids. The two fluids are subjected to a very high electrical current in the range of ~ 400 000 A and a magnetic field induced by the electric current of the range of 0.02 T [3].

Several studies are available in the literature on the flows in the electrolysis cell. Mathematical models are developed to investigate several impacts of velocity fields on its operation. The proposed models present flow simulations of the two fluids in three dimensions, where different physical phenomena are considered. Various works are carried out for the study of the generation of the bubbles in the electrolytic bath and the two-phase flow of the liquid and the gases [8-13]. Other studies have focused on the impact of flow on the dissolution of alumina in the bath [14]. The interface between the liquid aluminium and the electrolytic bath can be studied using 3D flow models [15, 16]. Simulations of the flow are also done in order to study and test the design of new cells [17-19] or for the study of its thermal balance [5, 20].

Mathematical modeling of 3D flows typically requires the use of turbulence models that take into account fluctuations in velocity over time and space. All the works cited above took into account a turbulence model in order to calculate the velocity field. However, very little information is available on the chosen model over another. In engineering, there are many different approaches for calculating turbulence for different applications [21]. The literature describes many case studies and validation scenarios of turbulence models in different applications, but very few are referring to the case of the electrolysis cell.

This work consists of the modeling of the flow of the fluids in the cell with a particular attention on the turbulence model to represent the velocity field fluctuations during electrolysis operations. The flow model is developed with the basic equations that govern the movement of fluids. Two approaches to represent turbulence are described and used in numerical simulations in order to compare the results. The two models to compare are Large Eddy Simulation (LES) and Reynolds Average Navier-Stokes (RANS). The comparison is made in order to see the viability of the two models to treat turbulence in the electrolysis cell. The hydrodynamic flow is modeled by using simplified conditions, but it is able to reproduce measured turbulence in the cell.

At the end, an attempt is made to compare the numerical results with some in-situ measurements made in an industrial electrolysis cell during its operation. The fluctuation of velocity over time was measured using the principle of drag force due to the flow of liquid aluminium around a body submerged in the aluminium layer.

2. Methods and Mathematical Model Description

The resolution of the equations governing the fluids is quite easily achievable according to numerical schemes available in the literature and such schemes are available in specialized CFD commercial codes. Large velocity fluctuations in the fluids are treated by the way of turbulence models in different industrial applications. Validation must be carried out in order to compare

the results of the different models with the velocity measured in the industrial cell during its operation.

Before performing a comparison with the measurement results, numerical comparisons can already show the different representations of turbulent flows and thus guide us to select a model for this kind of industrial application. This work aims to test mathematical models of turbulence in the cell.

Three models that have been used in the different works in flow modeling in the cell are part of the present study. A model of the Large Eddy Simulation Modeling (LES) family –Smagorinsky model – was chosen, as well as two models of the Reynolds Average Navier-Stokes (RANS) which are k-ε and the Renormalized Group k-ε (RNG k-ε). The choice of these models was based on the frequency of use of the two LES and RANS approaches and to verify and study their applicability to the fluid flow in the electrolysis cell.

2.1. Mathematical Equations

The domain considered in the mathematical model reproduces the geometry of a conventional cell used in industry with the industrial scale dimensions. Only the fluid domain is considered in the model in order to focus on flows only. The geometry was built using the ANSYS WORKBENCH® software and the domain mesh was made using the ANSYS DESIGN MODELER® module.

The phenomenological equations that govern the flows were calculated in the simulation domain using the ANSYS CFX® software in which we implemented different User Routine Functions where the body forces were linked to the momentum equations. This calculation code has already been used for the simulation of flows in the electrolysis cell [22]. It is a software specialized in Computational Fluid Dynamics based on the finite volume discretization approach [23]. To numerically simulate the flow of the liquid aluminium and the electrolyte bath, two immiscible liquid phases were considered in the volume of the domain. For each of the phases the equation of continuity was solved for the conservation of the mass considering the two liquids being incompressible as shown in Equation 1. The conservation of momentum is solved by taking into account the balance of external forces acting on the two fluids as shown in Equation 2.

$$\nabla \cdot u = 0 \tag{1}$$

with u the velocity of both fluids.

$$\frac{\partial(\rho u)}{\partial t} + \nabla \cdot (\rho\, u \circ u) = -\nabla p + \rho g + \nabla \cdot \tau + F_{Lz} \tag{2}$$

with p the pressure, τ the stress tensor, ρ the density and F_{Lz} the Lorentz force. The stress tensor is expressed in Equation 3.

$$\tau = \mu(\nabla u + \nabla u^T) \tag{3}$$

where μ is the dynamic viscosity and δ the identity matrix.

The Lorentz force expressed in Equation 4 is computed using the vector fields of the current density that crosses the two fluids $\vec{J}(J_x, J_y, J_z)$ and the magnetic field within the

domain $\vec{B}(B_x, B_y, B_z)$. More details on the boundary conditions and the origin of these vector fields are presented in subsection 2.3.

$$F_{Lz} = \vec{J} \wedge \vec{B} \tag{4}$$

The two immiscible liquid phases in the field of the cell were taken into consideration by means of the Volume of Fluids method (VOF). This method takes into account the density of each phase to consider buoyancy, as well as continuity at the boundary between the two phases, which constitutes the interface. The interface between the two fluids is tracked in all simulations. The cells of the elementary volumes which contain a volume fraction of 50 % of the two fluids were considered as the interface between the bath and the liquid aluminium. This method ensures the conservation of mass and momentum between the two fluids. As the two fluids are not allowed to mix and stratification is in effect all the time, the VOF method seems to be sufficient for monitoring the interface [24]. Equation 5 shows the VOF equation for both the phases.

$$\frac{1}{\rho_{Al}}\left[\partial_t(\alpha_{Al}\rho_{Al}) + \nabla.(\alpha_{Al}\rho_{Al}\vec{u}_{Al}) = \sum_{q=1}^{2}(\dot{m}_{Al\ bath} - \dot{m}_{bath\ Al})\right] \tag{5}$$

with ρ the density, α the volume fraction, $\dot{m}$ fluid flow in through an elementary volume and the index Al indicates the phase of aluminium and bath that of electrolyte. Equation 6 is the condition that the model must respect imperatively for the conservation of the two phases in the field since the model takes into account the two fluids (aluminium and bath).

$$\sum(\alpha_{Al} + \alpha_{Bath}) = 1 \tag{6}$$

As highlighted in the momentum conservation equation, the main forces to which both fluids are subjected are pressure forces, gravitational forces, shear forces and electromagnetic forces. The stratification is a consequence of the density difference of the two fluids as well as the diffusion between the liquid aluminium and the bath is negligible, so the mixing of both fluids is negligible in this context.

Both fluids are subjected to the stratified and free surface conditions with an atmospheric pressure at the top of the bath apart from the areas where the anodes are located. A central difference advection scheme is applied to the equation of motion. The simulations are transient in order to observe the fluctuation of the velocity as a function of time. Euler's second order backward transient discretization scheme is applied to the equation system. Regarding the source of motion, the Lorenz force is applied using an averaged scheme on elementary volumes.

2.2. Turbulence Models

In CFD, there are several turbulence models that have all been developed in order to solve flow problems with high degree of fluctuation of velocity. However, there are conditions of use of each type of model depending on the case studied. In the electrolysis cell, the flow of the two fluids has particular characteristics and is specific to this industrial application only. It is important to test different models in order to appreciate and see which model to apply and which one would be the most reliable for this case.

The most common model in numerical simulations is called RANS k-ε. It is therefore important to begin by applying it to the flow of fluids in the cell. As mentioned above, this model has been applied to the electrolysis cell with some uncertainty left regarding its reliability. In the k-ε model, an effective diffusivity is calculated by taking into account the velocity fluctuations around the average velocity. This approach highlights two new terms which are the kinetic energy of turbulence k and the dissipation rate ε which are solved by two partial differential equations, thus solving the equation system [24].

In the same family of RANS models, there exists a model called RANS RNG k-ε. This model takes into consideration the same principle as k-ε. Two partial differential equations are solved calculating the turbulence energy and the dissipation rate of the turbulence. The effective viscosity considered in the stress tensor is calculated as a function of the two parameters k and ε. The main difference between the two types of models lies in the estimation of the constants of the two partial differential equations. In the k-ε model, the two-equation constants are taken as constant values. More details on the constants are available in [25]. However, in the RNG k- ε model the turbulence energy equation remains the same, while for dissipation ε, a new term is added to the equation to make the model more suitable for vortical flows [26] as is the case in the electrolysis cell.

To have a broader comparison, the use of another model is important. The model of Large Eddy Simulation model has been chosen, particularly that of Smagorinsky [27]. The LES model is used to solve the Navier-Stokes equations for domains with large size-scales. In this case, the mesh used must be coarse due to the domain characteristics. The resolution of large-scale turbulence is done directly, while that of small scales or so-called SGS is modeled as a new viscosity term added to the viscous dissipation term. An algebraic function is used to distinguish the scales of magnitudes of the large scales of turbulence and that of the sub grid scales [28].

The simulations are performed to compare the amount of the computing resources and to identify the effect of parameters that define the turbulence of flows in different cases. The analysis performed consists of calculating the average velocity calculated by each model, the turbulent fluctuation, the turbulence strength and the turbulence intensity. Equations 7 to 10 show how these parameters are calculated:

$$\bar{u} = \frac{1}{N}\sum_{i=1}^{N} u_i \tag{7}$$

$$u' = u_i - \bar{u} \tag{8}$$

$$u_{rms} = \sqrt{\frac{1}{N}\sum_{i=1}^{N}\left(u_i'\right)^2} \tag{9}$$

$$\text{Intensity} = \frac{u_{rms}}{\bar{u}} \tag{10}$$

with u_i the calculated velocity for each time step i, $\bar{u}$ the algebraic mean velocity, u' the instantaneous velocity fluctuation, N the total number of time steps and u_{rms} the turbulence strength. The ratio $u_{rms}/\bar{u}$ represents the turbulence intensity. In order to see the spectrum amplitude of the velocity fluctuation a Fourier analysis is applied to the transient velocity values computed by the three models.

2.3. Body Force and Boundary Conditions

The body forces applied in the model are obtained from the data of a cell in operation and they consist of the current density as well as the magnetic field. These data are obtained using a proprietary mathematical model from Alcoa. The model developed in the present work calculates the forces from the current density and magnetic field distribution provided by the industrial partner. Figure 1 shows the contours of the Lorentz force in the cell domain as applied in the flow model. Figure 1 (a) shows the modulus of the electromagnetic force vector while Figure 1 (b) shows the magnitude of the horizontal component of the electromagnetic force.

(a)

(b)

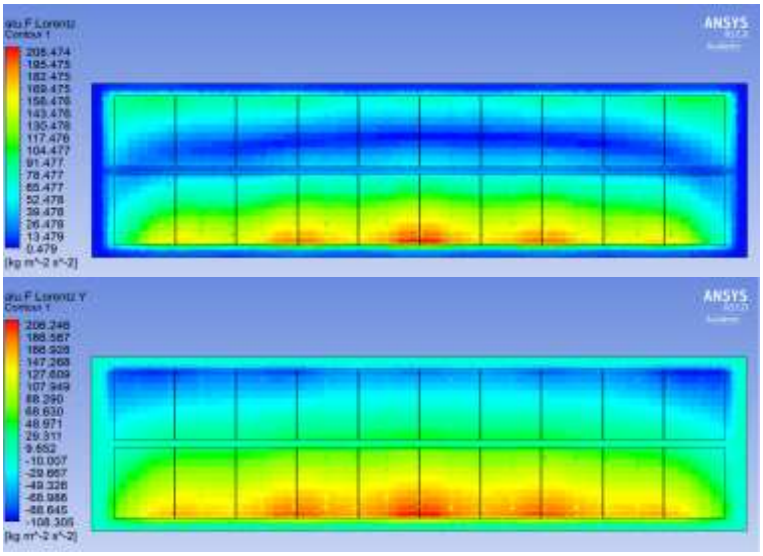

Figure 1. Contours of the electromagnetic force acting on the fluids in the cell: a) modulus of the Lorentz force and b) the horizontal component of this force.

The boundary conditions applied in the model were chosen to make the model simple to perform. Applied phenomena do not consider thermal and electrical physics. Only the hydrodynamics is considered. The conditions applied are the atmospheric pressure on the free surface of the cryolite bath and the suitable boundary layer function for each type of turbulence model.

2.4. Measuring the Velocity of the Liquid Aluminium in the Cell

Numerical simulations using different turbulence models provide a large amount of results that allow comparison between the results of each model. Measurements of fluid velocity in the electrolysis cell are important for further comparison between numerical and experimental results. Equipment for measuring the transient velocity of liquid aluminium in an operating electrolysis cell has been developed at the Aluminium Research Centre (REGAL) at Laval University. The equipment makes it possible to reach certain positions in the cell and to record the fluctuation of the liquid aluminium velocity in real time. Efforts have been made to design a measuring equipment that is suitable for chemically reactive medium at very high temperature. The probe limits flow disturbance during measurements and is sensitive enough to provide information on the velocity of liquid aluminium ten times per second. The manufacture of the assembly and the realization of the measurements follows the principles used in [29-32] and it is an objective of a master project conducted at Laval University [33].

3. Results and Discussion

The numerical simulations performed for this study were made over 600 s physical time from a static stratified state for the three turbulence models tested. The same domain has been tested with exactly the same conditions and the same grid of mesh. The meshing of the domain was studied in a previous work [34]. This gave altogether 21 030 317 elements. Transient simulations were obtained for time steps of 0.1 s. This time step coincides with the acquisition frequency of the apparatus which is used to record the fluctuations of the velocity as a function of time in the cell. From this basis, the comparisons made are reasonable and allow to give a solid idea about the behavior of the fluids in the cell using the different approaches of turbulence.

The results obtained made it possible to visualize the flow in any point of the field of the cell. The results presented in Figure 2 show the contours of the liquid aluminium velocity on the plane at 5 cm below the interface between the bath and the liquid aluminium. It is already evident from these results that the three models do not give exactly the same results on the amplitude and the distribution of the velocity field in the cell. The three approaches consider magnetic field induced turbulence work, but a direct and unverified application of a turbulence model could mislead the appreciation of the velocity results obtained, even if initially, the same conditions and motion sources are used in the model.

The choice of the position of the plane where the velocity contours are plotted corresponds to the height where the measurements were made. Figure 3 shows the position where the velocity of liquid aluminium was measured. This position corresponds to the area of the cell that was accessible, and where the tapping of aluminium is done. The numerical results of the liquid aluminium velocity simulation were recorded and analyzed at this position and compared with the measurement results.

(a)

(b)

(c)

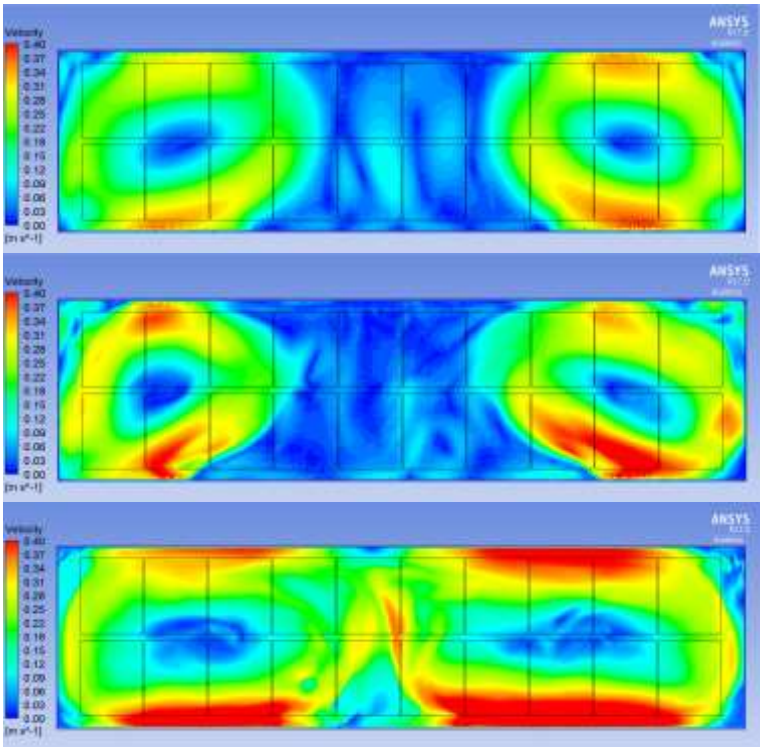

Figure 2. Velocity contours of aluminium at 5 cm below bath/aluminium interface a) LES Smagorinsky, b) RANS k-ε and c) RANS RNG k-ε.

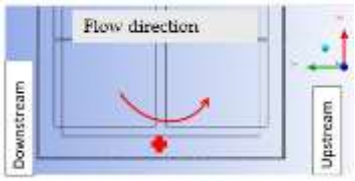

Figure 3. Recording position of the velocity fluctuation calculated by the model.

The simulations give the transient results of the velocity in 0.1 s intervals for a sufficient time to reach a pseudo-permanent flow. Since the simulations start from a static case, it is desirable to wait for the flow to be established and to see the amplitude of the fluctuations of the velocity. Figure 4 shows the results of the local transient velocity at the position shown in the previous figure. The traced velocities were obtained by LES Smagorinsky, RANS k-ε and RANS RNG k-ε in the three Figures 4 (a), (b) and (c) respectively. It can be seen that the local velocities calculated using the three turbulence models are different in relation to the amplitude of the fluctuations, even after the flow is established. The time averaged velocity at the point of measurement shown in Figure 3, calculated using the three turbulence models, is presented in Table 1. The predicted velocities remain in the same range between 22 and 28 cm/s. Although the approaches are different for calculating the flow velocity, the average velocities are still relatively close. Further analysis of the differences is needed.

Table 1. Time averaged local velocity at the point of measurement, calculated by the three turbulence models

	LES Smagorinsky	RANS k-ε	RANS RNG k-ε
Mean velocity [m/s]	0.22	0.26	0.28

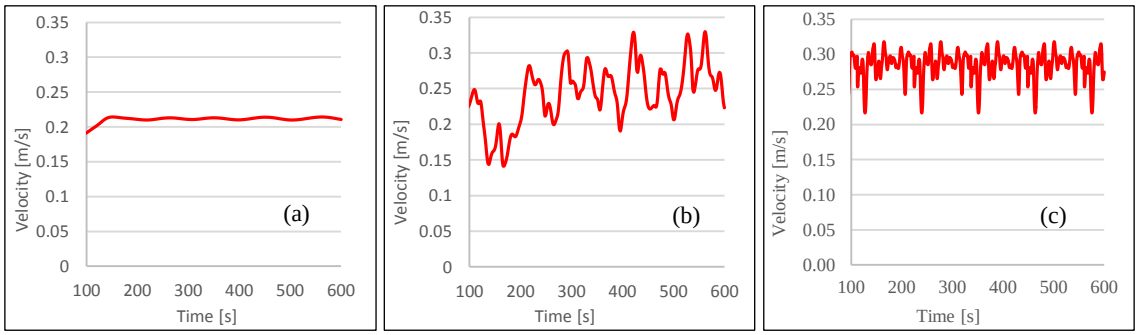

Figure 4. Local transient velocity calculated by the three models of liquid aluminium: a) LES Smagorinsky, b) RANS k-ε and c) RANS RNG k-ε.

Concerning the fluctuations of the velocity compared to the average velocity obtained by the different turbulence models, the results presented in Figure 5 (a), (b) and (c) show the fluctuation obtained for each model LES Smagorinsky, RANS k -ε and RANS RNG k-ε respectively. It is clear that for the first model LES Smagorinsky, the calculated fluctuation is small with a turbulence intensity of 0.8 %. For the two models RANS k-ε and RANS RNG, the calculated turbulence intensity are 13 % and 7 % respectively. Again, obvious differences between the three turbulence models are obtained, demonstrating the importance of selecting the representative turbulence model.

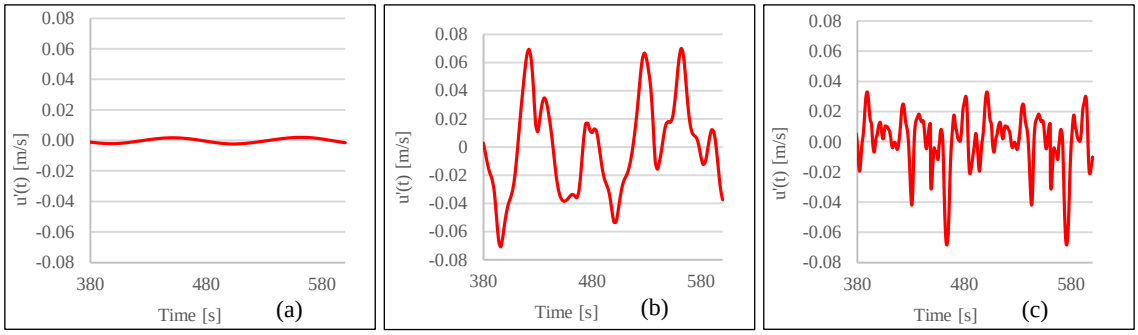

Figure 5. Transient fluctuation of the local velocity of Aluminium: a) LES Smagorinsky, b) RANS k-ε and c) RANS RNG k-ε

The results of the local velocity fluctuation compared to the average obtained with each of the models was analyzed by the Fourier transform. This analysis makes it possible to determine the frequency of each of the velocity fluctuations and thus to have information on the spectrum of the turbulence. Figure 6 shows the results of the frequency analysis of each of the turbulence models. The frequencies calculated by each of the models are in a relatively low frequency range. These values correspond to the fluctuation of the larger scales eddies, while the smaller scales are assimilated by the three models into the sub-grid scales. The three models differ strongly in the turbulence power spectrum.

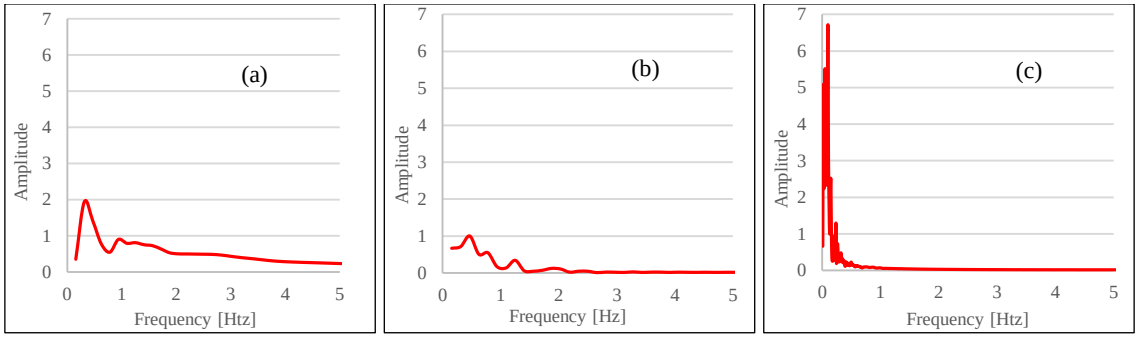

Figure 6. Fluctuation spectrum estimated by the three turbulence models: a) LES Smagorinsky, b) RANS k-ε and c) RANS RNG k-ε

Numerical simulations were performed on a 16-core compute cluster. It is important to present the practical side of the numerical investigations that have been done for the three models of turbulence. Since all the models chosen give relatively different results, their use must take into account the efforts related to each of the approaches as shown in Table 2.

Table 2. Duration of simulations performed by different turbulence models

Turbulence model	Duration of simulations
LES Smagorinsky	More than 3 weeks
RANS k-ε	Less than 3 days
RANS RNG k-ε	Less than 1 week

Measurements of the local velocity in the electrolysis cell were made at the same position where the results of the different turbulence models were recorded. Figure 7 (a) shows a sample of the velocity recorded using the measuring equipment developed. The velocity acquired by the probe makes it possible to record the two-dimensional velocity in the chosen position. Nevertheless, this velocity makes it possible to have an idea about the transient fluctuations of fluids velocity and this, at least in one position. Figure 7 (b) shows the magnitude of this fluctuation on which a

Fourier transform analysis has been applied. Figure 7 (c) shows the fluctuation spectrum of the flow.

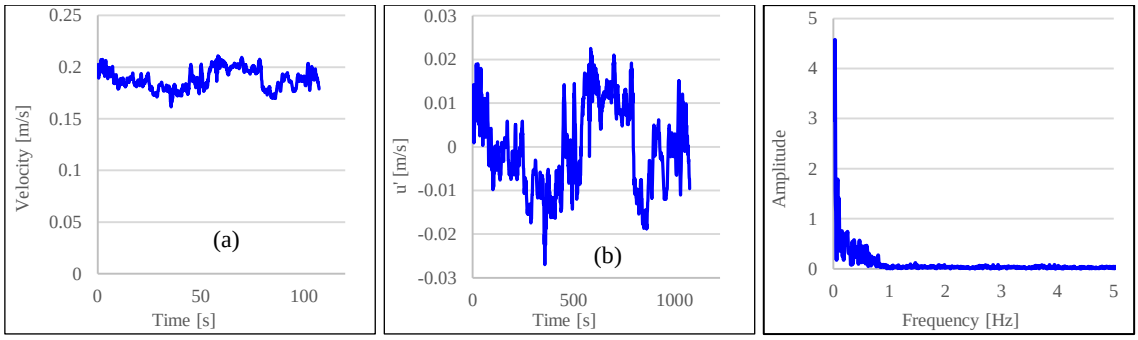

Figure 7. Measurement results sample of aluminium flow in the electrolysis cell: a) transient velocity, b) amplitude of the fluctuation and c) the frequency of the fluctuation.

Comparing the experimental results with that of the numerical simulations, several differences are highlighted. The average velocity over time at the specific location showed in Figure 3, obtained by the measurements is 18 cm/s, which is lower than that obtained by the three different turbulence models, given in Table 1. This may be because body force applied to the domain may be slightly different from the real conditions in the cell while the measurements are carried out. However, by comparing the fluctuations amplitude, the measurements show a maximum fluctuation of 2.6 cm/s which is comparable with the results obtained by the model RANS RNG k-ε.

The turbulence intensity obtained by the measurements is 5.5 %. This value is close to the turbulence intensity obtained by the RANS RNG k-ε model, i.e., 7 %. The comparison of the fluctuations spectrum presented in Figure 8 shows the differences in the amplitude of the velocity fluctuation frequency obtained by each model, with that obtained by the measurements.

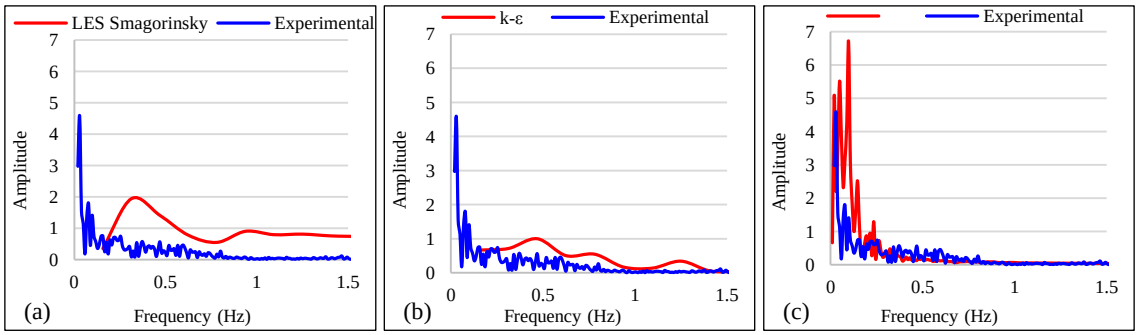

Figure 8. Comparison of the fluctuation amplitude frequency of the three turbulence models with that measured: a) LES Smagorinsky, b) RANS k-ε and c) RANS RNG k-ε.

4. Conclusions

Simulations with different turbulence models for bath and metal were performed using different approaches for the electrolysis cell. The results show that for the three models tested, the velocity ranges estimated at the end of the simulations are relatively comparable, but fluctuation magnitude and the frequency are quite different. Measurements in an industrial cell are valuable, while presently limited, and support slightly the use of the RANS RNG k-ε over the other turbulence models. The measurement system will be used widely in electrolysis cells under different conditions to analyse one-step ahead turbulence in aluminium electrolysis cell.

5. Acknowledgements

This work is carried out with the technical and financial support of Natural Sciences and Engineering Research Council of Canada (NSERC), ALCOA, Fonds Québécois de la Recherche sur la Nature et les Technologies (FQRNT), Aluminium Research Centre (REGAL) and Laval University. The authors acknowledge the technical and financial support of all the partners.

6. References

1 Halvor Kvande, 3 - Production of primary aluminium, Fundamentals of Aluminium Metallurgy, R. Lumley, Ed., 49-69: Woodhead Publishing, 2011.

2 François Charmier, Olivier Martin and Réné Gariépy, Development of the AP Technology Through Time, JOM, Vol. 67, no. 2, February 2015, 336-341.

3 Alton T. Tabereaux, and Ray D. Peterson, Chapter 2.5 - Aluminum Production, Treatise on Process Metallurgy, S. Seetharaman, Ed., Boston: Elsevier, 2014, 839-917.

4 S. R. Jakobsen et al., Estimating Alumina Concentration Distribution in Aluminium Electrolysis Cells, IFAC Proceedings Volumes, Vol. 34, No. 18, (2001), 303-308.

5 Dagoberto S. Severo, and Vanderlei Gusberti, A modelling approach to estimate bath and metal heat transfer coefficients, Light Metals 2009, 557-562.

6 Valdis Bojarevics, and Jim W. Evans, Mathematical modelling of Hall-Héroult pot instability and verification by measurements of anode current distribution, Light Metals 2015, 783-788.

7 Joakim Haraldsson, and Maria T. Johansson, Review of measures for improved energy efficiency in production-related processes in the aluminium industry – From electrolysis to recycling, Renewable and Sustainable Energy Reviews, Vol. 93, (2018), 525-548.

8 Knut Bech et al., Coupled current distribution and convection simulator for electrolysis cells, Essential Readings in Light Metals: Aluminum Reduction Technology, Volume 2, 2013, 396-401 (from Light Metals 2001, 463).

9 Kristian Etienne Einarsrud, Stein Tore Johansen and Ingo Eick, Anodic bubble behaviour in Hall-Héroult cells, Light Metals 2012, 875-880.

10 Zhiming Liu et al., Current efficiency predictive model and its calibration and validation, Light Metals 2012, 935-938, 2012.

11 Dagoberto S. Severo et al., Modeling the bubble driven flow in the electrolyte as a tool for slotted anode design improvement, Essential Readings in Light Metals: Aluminum Reduction Technology, Volume 2, 409-414, 2013 (from Light Metals 2007, 287-292).

12 Shuiqing Zhan et al., A CFD- PBM coupled model predicting anodic bubble size distribution in aluminum reduction cells, Light Metals 2014, 777-782.

13 Yiwen Zhou et al., Simulation of Anode Bubble: Volume of Fluid Method, Light Metals 2014, 783-788.

14 Yuqing Feng, Mark A. Cooksey, M. Philip Schwarz, CFD modelling of alumina mixing in aluminium reduction cells, Light Metals 2010, 543-548.

15 Jinsong Hua et al., Revised benchmark problem for modeling of metal flow and metal heaving in reduction cells, Light Metals 2014, 691-695.

16 Dagoberto S. Severo et al., "Comparison of various methods for modeling the metal-bath interface," Essential Readings in Light Metals: Aluminum Reduction Technology, Volume 2, 2013, 379-384 (from Light Metals 2008, 413-418).

17 Amit Gupta et al., Electromagnetic and MHD study to improve cell performance of an end- to- end 86 kA potline, Light Metals 2012, 853-858.

18 Zhiming Liu, Fengqin Liu, Yueyong Wang, Flow field comparison between traditional cell and new structure cell by CHALCO by CFD method, Light Metals 2012, 955-958.

19 Qiang Wang et al., Effect of innovative cathode on bath/metal interface fluctuation in aluminum electrolytic cell, Light Metals 2014, 491-494.

20 Kristian Etienne Einarsrud, Egil Skybakmoen, Asbjørn Solheim, On the influence of MHD driven convection on cathode wear, Light Metals 2014, 485-490.

21 Wolfgang Rodi, Turbulence models and their application in hydraulics, Routledge, 2017.

22 Dagoberto S. Severo et al., Modeling magnetohydrodynamics of aluminum electrolysis cells with ANSYS and CFX, Light Metals 2005, 475-480.

23 CFX-ANSYS, Release 11.0. Ansys CFX-Solver modeling Guide, ANSYS, Inc., 2009.

24 CFX-Solver-ANSYS, Theory Guide, Release ll, 2006.

25 Brian E. Launder, and D. Brian Spalding, The numerical computation of turbulent flows, Computer Methods in Applied Mechanics and Engineering, Vol. 3, No. 2, (1974), 269-289.

26 M. Lateb et al., Comparison of various types of k–ε models for pollutant emissions around a two-building configuration, Journal of Wind Engineering and Industrial Aerodynamics, Vol. 115, April 2013, 9-21.

27 J. Smagorinsky, General circulation experiments with the primitive equations: I. The basic experiment, Monthly Weather Review, Vol. 91, No. 3, (1963), 99-164.

28 M. Rieth et al., Comparison of the Sigma and Smagorinsky LES models for grid generated turbulence and a channel flow," Computers & Fluids, Vol. 99, 22 July 2014, 172-181.

29 R. Hernández-Walls et al., Design and calibration of an inexpensive digital anemometer, Physics Education, Vol. 43, No. 6, 2008, 593.

30 A. Moros, Drag anemometry for measuring velocities in electromagnetically driven flows, Journal of Physics E: Scientific Instruments, Vol. 19, No. 12, (1986), 1050.

31 C. Hopley, and M. Tunstall, A fast response anemometer for measuring the turbulence characteristics of the natural wind, Journal of Physics E: Scientific Instruments, Vol. 4, No. 7, 1971, 489.

32 A. Green et al., A rapid-response 2-D drag anemometer for atmospheric turbulence measurements, Boundary-Layer Meteorology, Vol. 57, No. 1-2, (1991), 1-15.

33 Samaneh Poursaman, Development of a drag probe for in-situ velocity measurement of molten aluminum in electrolysis cell, Master Thesis, Civil and Water Engineering Department, Laval University, 2018.

34 Mounir Baiteche *et al.*, "LES turbulence modeling approach for molten aluminium and electrolyte flow in aluminum electrolysis cell," *Light Metals 2017*, pp. 679-686: Springer, 2017.